AIAA 2003-3764

A Thermal Analysis Approach for the Mars Odyssey Spacecraft's Solar Array

John A. Dec and Ruth M. Amundsen
NASA Langley Research Center
Hampton, VA

36th AIAA Thermophysics Conference
23-26 June 2003
Orlando, Florida

A THERMAL ANALYSIS APPROACH FOR THE MARS ODYSSEY SPACECRAFT'S SOLAR ARRAY

John A. Dec and Ruth M. Amundsen
National Aeronautics and Space Administration
Langley Research Center
Hampton, VA 23681-2199

ABSTRACT

There are numerous challenges associated with placing a spacecraft in orbit around Mars. Often, trades must be made such as the mass of the payload and the amount of fuel that can be carried. One technique employed to more efficiently place a spacecraft in orbit while maximizing payload mass (minimizing fuel use) is aerobraking. The Mars Odyssey Spacecraft made use of aerobraking to gradually reduce its orbit period from a highly elliptical insertion orbit to its final science orbit. Aerobraking introduces its own unique challenges, in particular, predicting the thermal response of the spacecraft and its components during each aerobraking drag pass. This paper describes the methods used to perform aerobraking thermal analysis using finite element thermal models of the Mars Odyssey Spacecraft's solar array. To accurately model the complex behavior during aerobraking, the thermal analysis must be tightly coupled to the spatially varying, time dependent aerodynamic heating analysis. Also, to properly represent the temperatures prior to the start of the drag pass, the model must include the orbital solar and planetary heat fluxes. It is critical that the thermal behavior be predicted accurately to maintain the solar array below its structural flight allowable temperature limit. The goal of this paper is to describe a thermal modeling method that was developed for this purpose.

INTRODUCTION

The Mars Odyssey spacecraft was launched on a Delta II launch vehicle from Cape Canaveral Air Force Station on April 7th 2001. On October 23rd 2001, after a 197-day cruise, the spacecraft performed a propulsive maneuver to insert itself into an 18.5-hour elliptic orbit around Mars. To place itself into its 2-hour, 400km circular, sun-synchronous mapping orbit, Odyssey used the multipass aerobraking technique, the same technique utilized by the Magellan spacecraft around Venus and the Mars Global Surveyor spacecraft around Mars. Aerobraking makes use of atmospheric drag on each orbit pass to gradually reduce a spacecraft's velocity at periapsis, which then reduces the altitude at apoapsis. The Magellan spacecraft was the first three-axis stabilized spacecraft to perform this type of multipass aerobraking[1]. Mars Global Surveyor, the second to use multipass aerobraking, gradually reduced its orbit from an elliptic 45-hour period to about a 380km 2-hour circular orbit.

To control periapsis altitude, Magellan planned on using thermocouple data to signal the need to perform a periapsis raise maneuver, which would raise the periapsis altitude, lower the maximum atmospheric density experienced, and thus lower the aerodynamic heating on the spacecraft and solar arrays. In the literature, it was noted that Magellan experienced at least 5 thermal sensor failures prior to the start of aerobraking[2]. It is unclear from the available literature if any of these thermal sensors were located on the solar arrays and were to be used during operations. It is also unclear whether or not there were any thermal models developed and used during the Magellan aerobraking process to make up for the inoperable thermal sensors, but there are references to heat rate and surface temperature calculations being performed using a direct simulation Monte Carlo particle method[3,4]. In any event it is clear that in the early 1990's the limitations of computers would have prohibited the use of a sufficiently detailed finite element or finite difference model that could have been run in a timely enough fashion to be used during operations. During the Mars Global Surveyor operations, the heat rate encountered during previous drag passes was reconstructed using a 1-dimensional thermal model at various locations around the solar arrays. This model used the spacecraft and solar array thermal sensor temperature data as input to determine what heat rate the spacecraft and solar arrays experienced. A thermal model to predict the solar array temperatures for future drag passes and to reconstruct the solar panel temperatures for past orbits was not available. Originally, during operations, the plan for Mars Odyssey was to use a 1-dimensional thermal model similar to that of the Mars Global Surveyor model. Unlike Magellan and Mars Global Surveyor, Mars Odyssey was the first multipass aerobraking mission to make use of detailed 3-dimensional finite element thermal model during operations to predict the temperatures for future orbits and reconstruct the solar panel temperatures for past

orbits. This model, used in addition to the 1-dimensional model, provided detailed, 3-dimensional temperature profiles of the solar array, transient plots of maximum material temperatures, and transient plots of thermal sensor temperatures. It also provided the ability to identify the hottest spots on the solar array, and provided a means to develop thermal limits based on heat rate or atmospheric density.

THERMAL MODEL DEVELOPMENT

The thermal analysis of the solar array had three main components: the view factor and orbital heating analysis, the aerodynamic heating analysis, and the computation of solar array temperatures. The calculations were performed in two flight regimes. One regime was the vacuum phase where the spacecraft was in orbit around Mars, but out of the atmosphere. The thermal environment in this phase was dominated by the solar and planetary heating with negligible aerodynamic heating. The second regime was the aerobraking phase, or drag pass, where the spacecraft made its excursion into the atmosphere. The thermal environment in this phase was dominated by the aerodynamic heating (roughly 60 times greater than the orbital heating). Temperatures were calculated for both flight regimes. Accurate calculation of the solar/planetary flux during flight, as well as aerodynamic heating during drag passes, requires that the thermal analysis be tightly coupled to the flight mechanics, aerodynamics, and atmospheric analysis.

Solar Array Description

The function of Mars Odyssey's solar array is two-fold. First, its primary function is to provide a stable power source for the spacecraft and scientific instruments during all phases of the mission. Second, while in the stowed configuration, the solar array provides a large surface area on which the aerodynamic forces can act during each drag pass of aerobraking. Following Mars orbit insertion the Odyssey spacecraft begins aerobraking by slicing through the Martian atmosphere at a relative velocity of about 4.57 km/s. Despite low atmospheric densities of about 80 kg/km^3, these high velocities, along with the large exposed surface area, produce significant aerodynamic heating on the solar array, and spacecraft. Careful design and construction of the solar array allows it to withstand this aerodynamic heating.[6]

The Mars Odyssey solar array is a three panel, layered construction of low density materials. The panels are commonly referred to as the +X, -X, and mid panels. The +X and –X panels are mirror images of each other, while the mid panel has a unique geometry. Figure 1 shows a 3-dimensional geometric representation of the solar array. This geometric representation was developed in MSC/PATRAN and was used in the aerobraking thermal analysis. Each panel consists of five layers; the first three make up the structural components and provide the structural integrity during launch and throughout aerobraking. Specifically, the solar array structure is a sandwich construction with a 0.190mm (0.0075") facesheet of M55J/RS-3 graphite composite, a 19.05mm (0.75") 5052 aluminum honeycomb core, and another 0.190mm (.0075") M55J/RS-3 composite facesheet.

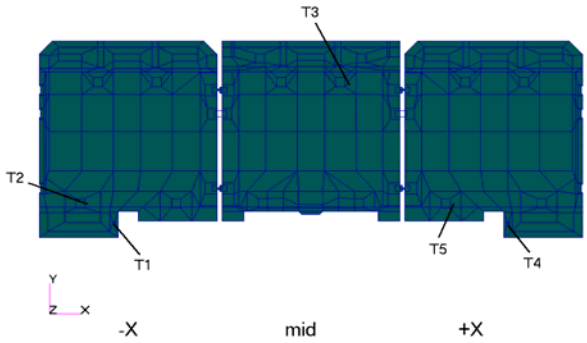

Figure 1. 3-D geometric representation of the Mars Odyssey solar array.

The next layer is a 0.051mm (0.002") Kapton sheet that is co-cured to the M55J/RS-3 graphite beneath it. The next layer is the solar cell layer and is made up of several sublayers: 0.190mm (0.0075") Gallium Arsenide solar cells, 0.152mm (0.006") cover glass, and 0.229mm (0.009") of adhesives[6]. Figure 2 shows a cross-sectional view of the solar array at a representative location.

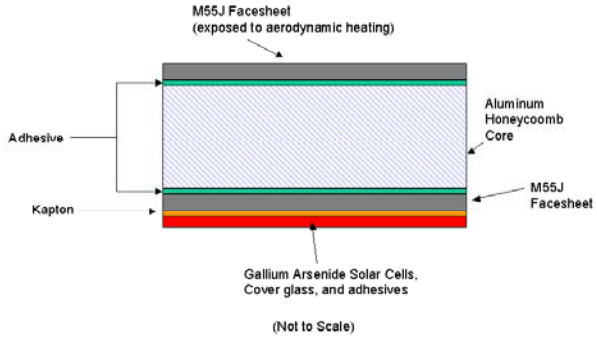

Figure 2. Cross-section of Mars Odyssey solar array

To reinforce certain areas of the array, sections of the standard 19.05mm (0.75") thick, 1.0 lb/ft^3 aluminum honeycomb core were replaced with a higher density core of the same thickness. Also, to reinforce the

array's hard points, a doubler sandwich structure was used. The doubler sandwich structure consisted of 0.381mm (0.015") layers of M55J/RS-3 graphite composite on either side of a 18.161mm (0.7125") aluminum honeycomb core. The doubler core densities varied depending on the location within the array and the expected loading in the region of concern. Examples of such reinforced hard points on the array are the hinge mounting points. Overall, the array design makes use of four different density aluminum honeycomb cores. Figure 3 graphically displays the locations of the different cores used and Table 1 lists the density and thickness of aluminum core used with respect to the colors in Figure 3. The table entries where the core thickness deviates from the nominal 0.75" thickness also show the locations of the M55J doublers. The doubler thickness is such that it brings the section back to the nominal panel thickness.

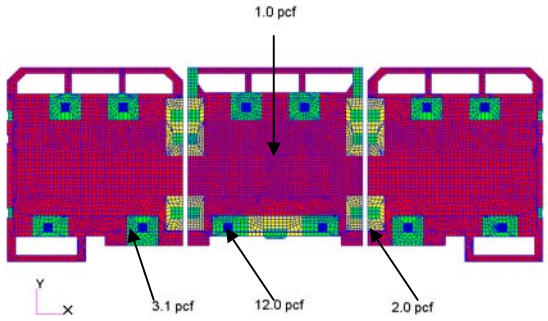

Figure 3. Variation in aluminum honeycomb core density (lb/ft^3)

Table 1. 5056 Aluminum honeycomb core

Marker	Density (lb/ft^3)	Thickness (in)
Red	1.0	0.75
Yellow	2.0	0.75
Green	3.1	0.715
Blue	12.0	0.715

To protect the array from aerodynamic heating, a 0.072mm (0.00283") thick layer of multilayer insulation (MLI) was placed on the facesheet exposed to the aerodynamic heating and around the edges of the M55J/RS-3 graphite facesheet. The bulk of the MLI was on the facesheet surface, and a small portion wrapped around the edges and terminated on the solar cell side. The width of the MLI on the solar cell side ranged from 50 – 148mm (1.96-5.83").

The solar array has five thermal sensors. There is one sensor on the mid panel on the solar cell side of the array. The +X and – X panels each have one sensor on the solar cell side and one on the "hot" facesheet side. On the engineering drawings[6], the thermal sensors are designated T1, T2, T3, T4, and T5. T1 and T4 are on the +/-X panel on the exposed facesheet side. T2, T3, and T5 are on the solar cell side; Figure 1 from above shows the locations of the thermal sensors on the solar array.

Orbital Heating Modeling

The orbital heating and view factor analysis, or radiation model, was performed using Thermal Desktop, a commercially available software package.[7] The radiation model was developed using engineering drawings of the spacecraft and solar array.[6] View factor and heat rate calculations were performed for several different solar array configurations and spacecraft orientations. First, calculations were made with the spacecraft and solar array in its vacuum phase configuration; the spacecraft oriented with its high gain antenna pointed towards Earth and the solar array normal to the sun. In transitioning to the aerobrake configuration, both heat rates and view factors to space for the solar array were calculated as the solar array articulated to its stowed position. As the spacecraft slewed to the aerobraking configuration, the solar array's view factors to space did not change, so view factors did not have to be recalculated for that maneuver.

Figures 4 and 5 show the spacecraft and solar array in the aerobrake configuration and vacuum phase respectively. This part of the analysis required detailed knowledge of the orbit and spacecraft orientation, and thus was highly dependent on the flight mechanics analysis. The orbital elements in the vacuum phase were obtained from a mission trajectory run-out performed by JPL[8]. For the drag pass phase, the orbital elements were obtained from POST simulations and output in unit vector form.

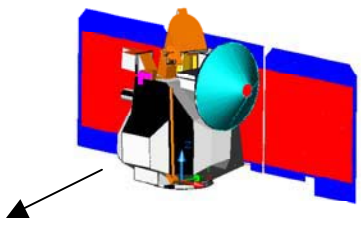

Figure 4. Mars Odyssey Thermal Desktop model in the aerobrake configuration.

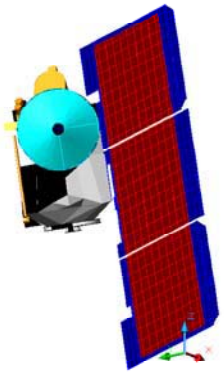

Figure 5. Mars Odyssey Thermal Desktop model in the vacuum phase configuration, view from Earth.

The vacuum phase orbital elements were input into Thermal Desktop via the "Keplerian Orbit" input option. This orbital input form requires the periapsis altitude, orbit eccentricity, right ascension of the sun, right ascension of the ascending node, and the argument of perigee. The vector output from POST is input into Thermal Desktop by using the "Vector List" orbit option where the user supplies the time, the unit x, y, and z components of the vector from the probe to the sun, and the unit x, y, and z components of the vector from the probe to the planet. The user also supplies the ratio of the distance to the spacecraft from the planet center and the planet radius. With the spacecraft removed for clarity, Figure 6 shows the view factors calculated with the solar array in the stowed, or aerobraking configuration. The view factors shown are for the facesheet exposed to the aerodynamic heating; the solar cell side has an unobstructed view to space so the view factor is equal to 1.0. Notice that the spacecraft prevents most of the middle panel from seeing deep space (low view factor); fortunately, the spacecraft also shields the middle panel from the aerodynamic heating thus, preventing a potential thermal problem due to inadequate radiative cooling.

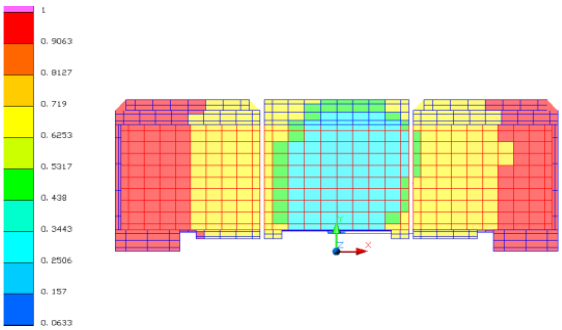

Figure 6. View factors to space for the facesheet exposed to aerodynamic heating in the aerobraking configuration.

Again with the spacecraft removed for clarity, Figure 7 shows a representative result of the solar/planetary heating near periapsis.

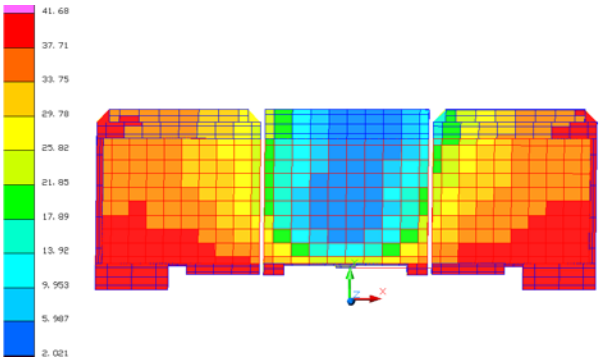

Figure 7. Typical orbital heat flux near periapsis on the facesheet exposed to aerodynamic heating in the aerobraking configuration. (W/m^2)

After completing the orbital heating and view factor calculations, this data had to be input into PATRAN Thermal for use in the temperature calculations. This process will be explained in detail later in the boundary conditions and data exchange section.

Aerodynamic Heating Analysis

The aerodynamic heating analysis consisted of calculating the atmospheric density, the spacecraft velocity relative to the atmosphere, and the heating coefficient for points spatially across the array. Using this information, the incident aerodynamic heating was calculated using equation 1,

$$Q_i = \frac{1}{2} \cdot \rho \cdot V^3 \cdot C_H \qquad (1)$$

where ρ is the atmospheric density, V is the relative velocity, and C_H is the heat transfer coefficient. This calculation was made at 5-second intervals throughout the aerobraking pass to give a transient representation of aerodynamic heating. A database of the heat transfer coefficients was developed using a Direct Simulation Monte Carlo (DSMC) particle method -- specifically the programs DAC and DAC free were used. From the POST simulations, the flight mechanics team was able to provide the atmospheric density and the relative velocity as a function of time (during operations, to reconstruct past orbits, the density was calculated using acceleration readings from the flight accelerometer)[9]. Using the density and the relative atmospheric velocity, the heating coefficients were calculated. Due to the long run times needed to perform the DSMC computations, an aerothermodynamic database was

developed prior to aerobraking. Then for each time step, the density was calculated by interpolating on either the accelerometer data, or the calculated density versus time output from POST. For both cases, the heating coefficients across the array were calculated by interpolating between density and relative velocity. The interpolation error on the heating coefficients was calculated to be about 2%, which was within the accuracy of the DSMC calculations. The heat transfer coefficients ranged from a peak value of 0.90 to a low value of 0, and included the surface accommodation coefficient.

Reflected heat is a phenomenon which occurs when particles striking the surface of the solar array leave the surface with more energy. This occurs when the surface temperature of the solar array has increased enough to impart some of its thermal energy to incident particles which are at a lower energy level. The thermal model accounts for reflected heat, which was approximated empirically for this mission using equation 2 and is a function of the incident heat flux and surface temperature.

$$Q_{ref} = \tfrac{1}{2}\rho V^3 \left[0.015 + 0.1\left(1 - \frac{Q_i}{\tfrac{1}{2}\rho V^3} \right) \right] \cdot \left(\frac{T_{wall}}{300} \right) \quad (2)$$

where T_{wall} is the surface temperature of the solar array. Equations 1 and 2 reveal the coupling of the thermal analysis to the flight mechanics, aerodynamics and atmospheric analysis. These calculations provided an accurate representation of the aerodynamic heating as well as reflected heating that was a function of time as well as position on the solar array.

Temperature Calculations

The temperatures for the solar array were calculated with the commercially available software MSC/PATRAN Thermal[10]. Like the Thermal Desktop model, a 3-D model of the solar array was developed solely using engineering drawings[6]. Normally, it is less efficient to create two thermal models, however, since existing FORTRAN code would allow simple inclusion of the aeroheating fluxes in PATRAN and because existing methods could be easily applied[11], this inefficiency was nullified. Also, the Thermal Desktop radiation model was necessary since orbital heating capabilities do not exist within MSC/PATRAN.

The PATRAN model represented all three solar panels, and included both facesheet layers, the aluminum honeycomb core, the Kapton, the MLI, and one layer for the solar cells. The solar cell layer included the cover glass, wire, solder, and adhesives that were modeled as an averaged mass spread evenly across the layer. This was an engineering approximation since the wire, solder, etc., were not evenly distributed across the panels. The titanium hinges and dampers that physically connect the three solar panels were also included in the model and provided a thermal link between the three panels. The model was highly detailed and included the variations in the aluminum honeycomb core density as well as the varying thickness of M55J composite facesheet doublers. For all materials, properties were included as functions of temperature; for the aluminum honeycomb core and M55J facesheets, orthotropic material properties were included. The five spacecraft thermal sensors were modeled as bar elements which had mass and were thermally connected to the spacecraft with a contact resistance. Overall, the PATRAN thermal model was a physically accurate 3D representation of the solar array. Compared to the as-built mass of the solar array of 32.3 kg, the mass of the PATRAN thermal model was 33.4 kg, a difference of only 3.4%.

The PATRAN thermal model required input boundary conditions from the two analysis components mentioned earlier. The model included radiation to space, incorporating the view factors that were calculated from Thermal Desktop. The orbital and planetary heat fluxes calculated from Thermal Desktop were applied to the surfaces of the model as well. The aerodynamic heating and reflected heating boundary conditions were applied to the exposed M55J facesheet and MLI surfaces. Heating on the edges of the panels was included as 5% of the incident heating of the nodes closest to the edge. Edge radiation was included around the outer-most edges with a view factor to space of 1.0. Radiation back to the spacecraft bus was included, with the spacecraft bus simply modeled as a node with a constant temperature.

Boundary Conditions and Data Exchange

The process of applying the aerodynamic heat loads, orbital heat loads, and integrating the view factors from Thermal Desktop into PATRAN was developed for Mars Global Surveyor[11]. These processes had to be modified slightly to accommodate the Mars Odysseys solar array configuration and simplified slightly to be of use during Odysseys' operations phase.

The process of applying the aerothermodynamic heat loads calculated by DAC to the PATRAN thermal model involved the use of a MATLAB script and customized FORTRAN program that interfaced with the PATRAN solver at run time. Incorporating the view factors and orbital/planetary heat loads calculated

by Thermal Desktop did not require the use of the customized FORTRAN code or the MATLAB script, but did require several preprocessing steps in order to import the data into PATRAN. The MSC/PATRAN Thermal user's guide[10] describes how to incorporate user supplied FORTRAN subroutines, and therefore it will not be discussed here. However, the process and flow of data from the aerothermodynamic database to the PATRAN thermal model will be described. As mentioned previously, an aerothermodynamic database was developed prior to the start of Odyssey's aerobraking. This database consisted of a spatial map of the heat transfer coefficients over the array as a function of atmospheric density and relative velocity. The drag pass duration, which defined the length of the transient in the thermal model, was provided by the flight mechanics team. Along with the drag pass duration, they provided a time history of the atmospheric density and relative velocity, the time interval of which was five seconds. Prior to the execution of the PATRAN thermal analysis, the MATLAB script was executed. The MATLAB script read the density, and relative velocity data, as well as the aerothermodynamic database, and for each time interval performed an interpolation over density and relative velocity to obtain the spatial heating distribution. The MATLAB script's output was a file that contained blocks of data with the time interval as a heading for each block, and a table of X, Y, and Q, where X and Y are the spatial coordinates of the DSMC grid and Q is the incident heat flux calculated by equation 1. Upon execution of the PATRAN thermal analysis, the PATRAN solver makes a call to the customized FORTRAN subroutine. The subroutine performs an initialization by reading the MATLAB output file and storing the data in a three dimensional array. The first two indices for the array are the number of X and Y points on the DSMC grid. The third index is a time index with its maximum value equal to the number of output time points provided in the density/relative velocity data. With this initialization procedure complete the FORTRAN subroutine passes back control to the PATRAN Thermal solver, where it begins its iterative solution process. For every time step in the solution and at every node location that was flagged as having incident aerodynamic heating, the PATRAN solver makes a call to the FORTRAN subroutine. The subroutine then performs two interpolations. The first is an interpolation over time to obtain the heating at the correct time in the trajectory. The second interpolation is over X and Y to obtain the heating for the current node, since the x and y locations for the PATRAN nodes differ from the DSMC grid node locations. The FORTRAN code passes the nodal heat rate back to the PATRAN solver and the solution process continues until convergence is obtained. Once the solution converges, the solver moves to the next time step and the process is repeated. Figure 8 shows the DSMC data mapped to the PATRAN model with the final result of equation 1 plotted.

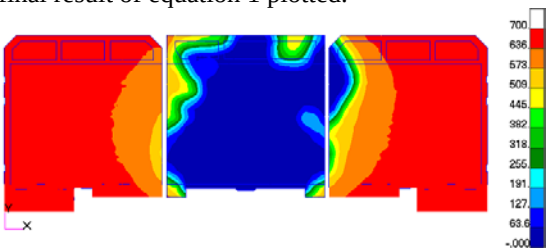

Figure 8. Example of aerodynamic heating mapped to the PATRAN model (W/cm^2).

The process for importing Thermal Desktop data into PATRAN Thermal is not straightforward and is labor intensive. First, a nodal position report must be created from within PATRAN. This report is nothing more than a text file that contains the node number, X, Y, and Z locations of the nodes. The nodes selected for inclusion in this report are associated with the surfaces in the thermal model that have the radiation boundary condition imposed on them. Since the physical location of the solar array with respect to the coordinate system is different in the PATRAN and Thermal Desktop models, some corrections to the nodal coordinates had to be made. These corrections were made in Microsoft Excel and saved as a new text file. The disconnect in the physical location of the array was due to the fact that the spacecraft bus was modeled in Thermal Desktop, but was not modeled in PATRAN. In Thermal Desktop, the origin was the center of the spacecraft, and in PATRAN, the origin was along the bottom edge of the array at the midpoint of the middle panel. Once the corrected nodal position report is acquired, the Thermal Desktop model is run to solve for the view factors to space and the orbital heat rates. Utilizing the internal interpolation routine in Thermal Desktop called "map data to locations", the PATRAN nodal position report is supplied as input and Thermal Desktop produces a text file that includes the PATRAN node number and the mapped Thermal Desktop data. This file then needs to be imported into PATRAN as a spatial field. This is accomplished by using the spreadsheet utility in PATRAN. To import the data, simply start the spreadsheet utility in PATRAN, then using standard windows file open procedures, open the Thermal Desktop data file. The opening procedure loads the data into the spreadsheet, then an internal PATRAN spreadsheet function is used to create a field from the spreadsheet data. The field generated is a finite element field and can be used as the input for the "Form Factor" entry in the gap radiation boundary condition dialog box. All of the radiation boundary

conditions to space were created in this way. Figure 9a shows the view factors to space in the Thermal Desktop model and Figure 9b shows the view factors as mapped to the PATRAN model. A similar procedure is followed to import the heat rate data from Thermal Desktop to PATRAN. This procedure becomes cumbersome if the heat rates vary greatly over an orbit, or if the view factors change, as is the case when the spacecraft slews and stows the solar array prior to a drag pass. To include these changes, the transient prior to the start of the drag pass had to be broken into stages. Each stage was solved independently and each successive stage used the previous stage's final temperatures as its starting temperature. The only exception was the first stage where the steady state temperatures were calculated for the solar array in the vacuum phase prior to the start of the slewing and stowing operations. The temperatures calculated by the final stage before the drag pass began were used as the initial solar array temperatures for the start of the drag pass.

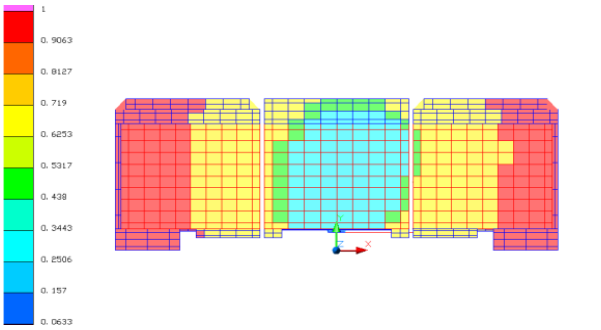

(a)

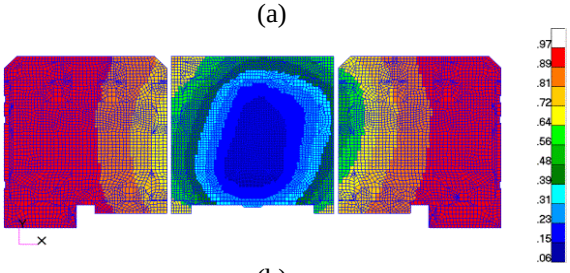

(b)

Figure 9. View factors to space: (a) Thermal Desktop, (b) mapped to PATRAN

The temperatures obtained prior to the drag pass were primarily dependent on the orbital heat rates and view factors calculated from Thermal Desktop, but most significantly, they were influenced by the fact that the spacecraft passed into solar occultation and was shaded by Mars on average, for about 4 minutes before the drag pass began. This reduced the initial temperatures and allowed the solar array to absorb more energy and therefore increased the margin between the flight temperatures and the thermal limits. Finally, during the drag pass, a transient analysis was performed to determine the temperatures, where the aerodynamic heating was dominant. Temperature predictions were made prior to each drag pass and temperatures were calculated using actual spacecraft telemetry to reconstruct past orbits.

TEMPERATURE PREDICTIONS

The initial goal of the thermal analysis was to provide an independent validation and verification of the analysis already being performed on the solar array. This included verifying the location and magnitude of predicted hot spots on the array, and verifying the solar array's thermal limit. The thermal limit is expressed in terms of the heat flux level and is that heat flux which would cause the solar array to exceed its flight allowable temperature of 175°C. The high fidelity nature of this 3-dimensional analysis, and the speed at which analysis results could be produced, were compelling evidence to include this analysis in the trajectory decision making process during aerobraking operations. However, in order for the analysis to be useful during operations, temperatures needed to be calculated and post processed within 4 hours.

Utilizing a 1.7GHz dual XEON processor computer made it possible for this highly detailed finite element analysis to run in about one hour. Although, as drag pass duration increases, so does the run time. This increase was slight, and for the longest drag passes the solution time never exceeded 1 hour 15 minutes. Computer speed alone was not the only means of increasing efficiency. The spacecraft's configuration in the vacuum phase was always the same so vacuum phase temperatures remained virtually constant. Also, the occultation duration changed very slowly, causing the initial temperatures to change at a slow, predictable rate. Therefore, to increase analysis efficiency, the view factor, orbital heating, and vacuum phase temperature analyses could be performed on an as-needed basis.

The thermal analysis was highly dependent on all of the other analyses being performed. Any problems arising within another group's analysis caused delays in the completion of the thermal analysis. This highly detailed thermal model generated a large quantity of information about the thermal state of the solar array. Figure 10 shows the predicted temperature distribution for orbit pass 40, just after periapsis, which is typical of the majority of the drag passes encountered. This temperature distribution was calculated using a predicted density, and velocity profile, and assumed a nominal orientation relative to the atmosphere. Figure 11 shows the predicted temperature of the thermal

sensors and the predicted heat rate as a function of time centered on periapsis.

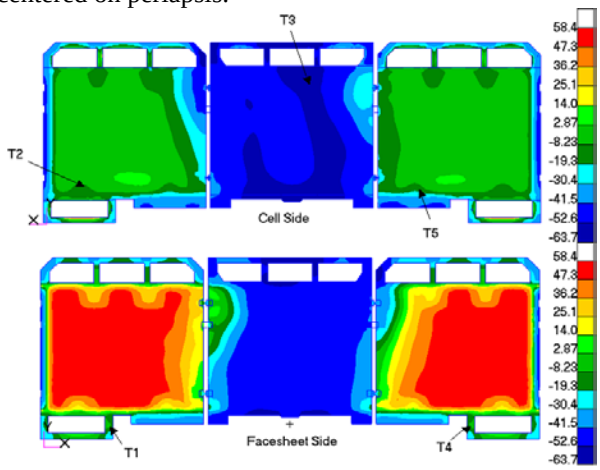

Figure 10. Predicted temperature distribution on the solar array for orbit pass 40.

A similar transient plot was generated for each material, where the maximum predicted temperature for any location on that material is tracked. Figure 12 shows the maximum material temperatures as a function of time.

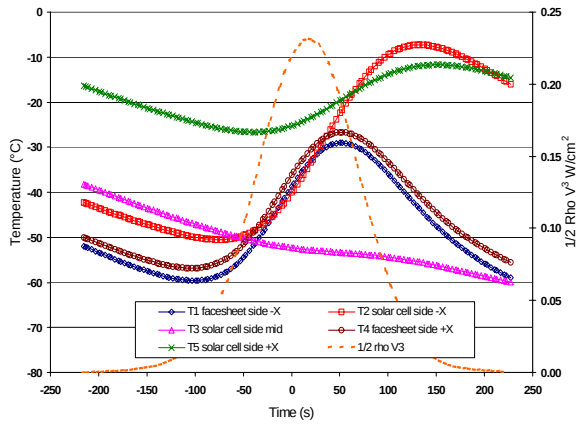

Figure 11. Thermal sensor temperature predictions, orbit pass 040, peak heat flux = 0.232 W/cm^2.

This plot differs slightly from the plot of the thermal sensor temperatures. The obvious difference is that the maximum material temperatures are significantly higher than the predicted thermal sensor temperatures. In the case of the M55J graphite, which was exposed to the flow, the figures show that the peak temperature was 85°C higher than the peak on either of the facesheet thermal sensors, T1 and T4. This was a result of having MLI covering the facesheet in the areas near those thermal sensors. The MLI provided sufficient shielding to the underlying material from the incident heat flux to prevent the material in those regions from reaching higher temperatures. Throughout the main phase of aerobraking, the magnitude of the temperature difference between the material maximum and the thermal sensor maximum was dependent on the heat flux, and the difference grew as the magnitude of the heat flux grew.

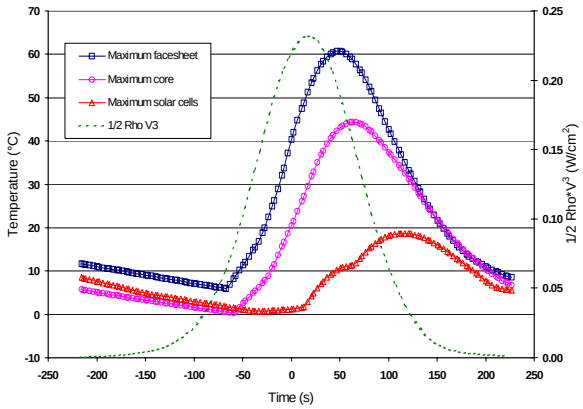

Figure 12. Maximum predicted material temperatures, orbit pass 040, peak heat flux = 0.232 W/cm^2.

In all of the trajectories that were encountered, the material maximum was always higher than what the thermal sensors indicated and was always located in the lower, outboard quadrant of the +X panel. Another minor difference between the thermal sensor and maximum material temperature plots is due to the fact that the location of the maximum material temperature changed throughout the drag pass. In Figure 12 where there seem to be discontinuities and the temperature seems to jump, the maximum temperature shifts to another node in that particular material layer.

In Figures 11 and 12, the heat rate is represented by a smooth gaussian like profile. The heating is directly proportional to the atmospheric density; the density predictions, which came from an Odyssey version of Mars GRAM 2000, do not account for atmospheric density variations and thus have an average density profile as a function of altitude. Large uncertainties in predicting the atmospheric density from orbit to orbit made the temperature predictions less valuable than expected, but they were still useful in that they gave a 3-dimensional picture of the thermal state of the array, and could identify any thermal anomalies.
Although the uncertainties in the density predictions were present, they did not impact the prediction of the thermal limit lines, which turned out to be a very useful tool. The flight corridor for main phase aerobraking was chosen based on the maximum Q dot, which was the value of the aerodynamic heating that would cause the solar array to exceed its flight allowable temperature limit for the structure of 175°C. The upper

flight corridor was reduced by a factor of 2 to carry 100% margin with respect to the limit. Figure 13 is a plot of the maximum solar array temperature as a function of Q dot, covering orbit passes 77 through 99. This plot was generated by running the PATRAN thermal model with varying density and hence heating profiles. Four different density profiles were used: the low, middle, and upper ends of the flight corridor, as well as one that would produce a maximum Q dot of 0.8 W/cm^2. A Q dot of 0.8 W/cm^2 was chosen as the upper bounding case because it guaranteed the solar array prediction would exceed the flight allowable temperature of 175°C. By using a predicted Q dot, or one derived from flight data, the JPL Navigation team could quickly determine the maximum predicted temperature of the solar array. Determining the thermal limit of the solar array in terms of the Q dot was obtained simply by finding the value of Q dot that corresponded to 175°C. Figure 13 is a snap shot of temperature vs, Qdot over a small interval. This same process could be repeated for several orbit trajectories, and a mission thermal limit line could be generated. Figure 14 shows the limit line as determined by the PATRAN thermal model plotted as a function of apoapsis altitude. The two limit lines show how significant the allowable temperature is in determining the thermal limit of the array. Simply increasing the flight allowable temperature to 190°C will increase the thermal limit by about 10%. As the mission progressed the correlation of the thermal model to flight data improved significantly. Since the thermal model and limit lines were updated continuously based on the correlations, confidence in the limit line chart increased dramatically during operations.

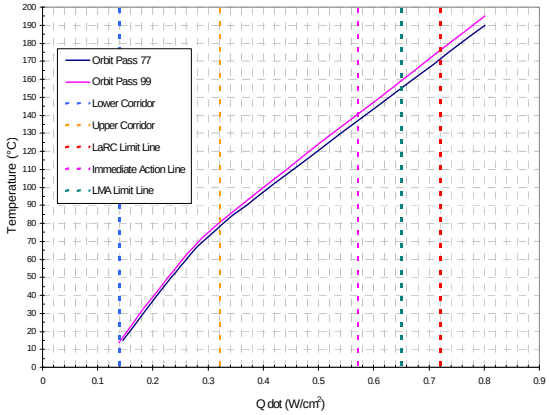

Figure 13. Temperature as a function of Q dot and orbit pass.

In figure 13 there are two limit lines: one is a limit line based on the NASA Langley 3-dimensional finite element thermal model, and the other is the limit line calculated by Lockheed Martin's 1-dimensional model of the solar array. The Lockheed limit line was more conservative and as such was used as the flight maximum.

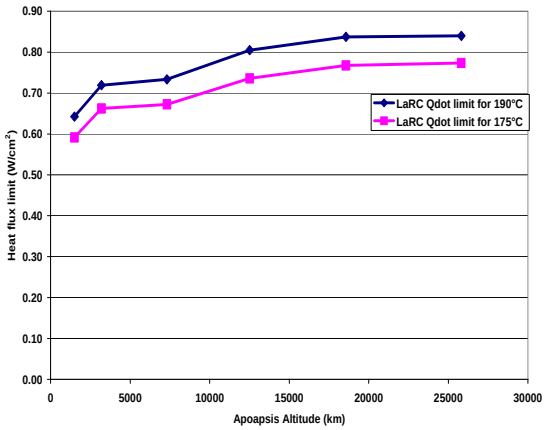

Figure 14. Thermal limit line encompassing the entire mission.

CONCLUSIONS

It has been shown that a 3-dimensional finite element model developed to represent the actual flight hardware of the Mars Odyssey solar array can be used without a significant run-time penalty. The detail captured and the quantity of data generated by such a high fidelity model is not possible using a 1-dimensional model alone. The 3-dimensional model showed that the hot spots were not located near any of the flight thermal sensors. It is believed that such a high fidelity model, used earlier in the design phase, could identify the hot spots and be used to place thermal sensors where they are most needed. Also, the 3-dimensional model demonstrated that it could be used to evaluate and establish the thermal limit lines for the solar array in both the design and operational phases. By applying lessons learned and using existing methods and processes the model development time was drastically reduced while the overall quality of the thermal models increased.

ACKNOWLEDGMENTS

The authors would like to thank Richard Kriegbaum of Lockheed Martin Astronautics for providing drawings, details of the assembly, and advice. Also, thanks go out to the JPL navigation team for giving us the opportunity to make a contribution to this mission. We would also like to thank Mike Lindell for providing supporting structural analysis.

REFERENCES

[1]Carpenter, A. S., "The Magellan Aerobraking Experiment: Attitude Control Simulation and Preliminary Flight Results", AIAA Paper 93-3830, August 1993.

[2]Neuman, J. C., Buescher, J. A., and Esterl, G. J., "Magellan Spacecraft Thermal Control System Design and Performance", AIAA 28th Thermophysics Conference, Orlando, Florida, AIAA 93-2844, July 6-9, 1993.

[3]Haas, B. L., Feiereisen, W. J., "Particle Simulation of Rarefied Aeropass Maneuvers of the Magellan Spacecraft", AIAA 27th Thermophysics Conference, Nashville, Tennessee, AIAA 92-2923, July 6-8, 1992.

[4]Haas, B. L., Schmitt, D. A., "Simulated Rarefied Aerodynamics of the Magellan Spacecraft During Aerobraking", AIAA 93-3676-CP, July 6-9, 1993.

[5]Beerer, J., et. al., "Aerobraking at Mars: The MGS Mission", AIAA 34th Aerospace Sciences Meeting and Exhibit, Reno, Nevada, AIAA 96-0334, January 15-18, 1996.

[6]Engineering Drawings from Lockheed Martin (919M0000020), SpectroLab Inc. (041312-041314), and Spectrum Astro Inc. (AM 111372-001, -002, -003) Various release dates 1997-1998.

[7]Thermal Desktop User's Manual, Version 4.4, Cullimore & Ring Technologies.

[8]Email from JPL with excel spreadsheet attachment containing mission run-out orbital elements.

[9]Dec, John A., Gasbarre, Joesph, and George, Benjamin, E. LT., "Thermal Analysis and Correlation of the Mars Odyssey Spacecrafts' Solar Array During Aerobraking Operations", AIAA 2002 Astrodynamics Conference, Monterey, California, AIAA 2002-4536, August 2002.

[10]MSC/PATRAN Thermal User's Guide, Version 2000r2 MSC Software.

[11]Amundsen, Ruth M., Dec, John A., and George, Benjamin, E. LT., "Aeroheating Thermal Model Correlation for Mars Global Surveyor (MGS) Solar Array", AIAA 2003 Thermophysics Conference, Orlando, Florida, June 2003.